Ubiquitylation of the nuclear pore complex controls nuclear migration during mitosis in *S. cerevisiae*

Akira Hayakawa,[1] Anna Babour,[1] Lucie Sengmanivong,[2,3] and Catherine Dargemont[1]

[1]Institut Jacques Monod, University Paris Diderot, Sorbonne Paris Cité, Unité Mixte de Recherche 7592, Centre National de la Recherche Scientifique, Cedex 13, 75205 Paris, France
[2]Cell and Tissue Imaging Facility and [3]Nikon Imaging Center, Research Unit 144, Curie Institute-National Center for Scientific Research, Cedex 05, 75248 Paris, France

Nuclear pore complexes (NPCs) correspond to large protein transport complexes responsible for selective nucleocytoplasmic exchange. Although research has revealed much about the molecular architecture and roles of the NPC subcomplexes, little is known about the regulation of NPC functions by posttranslational modifications. We used a systematic approach to show that more than half of NPC proteins were conjugated to ubiquitin. In particular, Nup159, a nucleoporin exclusively located on the cytoplasmic side of the NPC, was monoubiquitylated by the Cdc34/SCF (Skp1–Cdc53–F-box E3 ligase) enzymes. Preventing this modification had no consequences on nuclear transport or NPC organization but strongly affected the ability of Nup159 to target the dynein light chain to the NPC. This led to defects in nuclear segregation at the onset of mitosis. Thus, defining ubiquitylation of the yeast NPC highlights yet-unexplored functions of this essential organelle in cell division.

Introduction

The nuclear pore complex (NPC) is the unique selective gate for the bidirectional transport of macromolecules across the nuclear envelope. NPC is also one of the largest assemblies of defined structure in the cell, with a size of ∼50 MD. NPCs are common to all eukaryotes and are composed of ∼30 distinct nucleoporins (Nups), a broadly conserved set of proteins that have been fully cataloged in both yeast and vertebrates (Rout et al., 2000; Cronshaw et al., 2002; Alber et al., 2007). NPCs are organized in five distinct substructures composed of precise Nups subcomplexes and corresponding to specific locations and functions. The membrane ring composed of transmembrane proteins anchors the NPC in the nuclear envelope, whereas outer and inner rings form the NPC core scaffold and are connected by linker Nups. Nups containing FG (phenylalanine/glycine) repeats are mainly responsible for the transport function of the NPC by mediating interactions between the NPC and transport receptors (Alber et al., 2007).

Although research has revealed much about the molecular architecture and roles of the NPC subcomplexes, little is known about the regulation of NPC functions by posttranslational modifications. Phosphorylation of Nups by mitotic kinases, including Cdk1 or NIMA-related kinases, has been proposed to mediate NPC disassembly during prophase (Macaulay et al., 1995; Glavy et al., 1997, 2007; Onischenko et al., 2005; Lusk et al., 2007; Laurell et al., 2011). Function of the NPC in nuclear transport is also regulated via phosphorylation of FG-Nups by extracellular signal–regulated kinase (Kosako et al., 2009). In higher eukaryotes, Nup96 is ubiquitylated and degraded by the proteasome in a cell cycle–dependent manner (Chakraborty et al., 2008). High-throughput datasets of ubiquitylated proteins only identified some yeast Nups as being modified (Nup84, Nup145, Nup120, Nup157, Nup60, and Nic96) without validation nor precise information on the extent of ubiquitylation and functions of such modifications (Hitchcock et al., 2003; Peng et al., 2003).

In this work, we systematically analyze ubiquitylation of the yeast NPC and find that more than half of NPC proteins are conjugated to ubiquitin. These modifications are not simply related to proteasome-dependent protein turnover of the NPC but, as exemplified by Nup159 ubiquitylation, participate to the cell cycle progression.

Correspondence to Catherine Dargemont: dargemont.catherine@ijm.univ-paris-diderot.fr

Abbreviations used in this paper: NPC, nuclear pore complex; Nup, nucleoporin; SIM, structured illumination microscopy; wt, wild type.

The Rockefeller University Press $30.00
J. Cell Biol. Vol. 196 No. 1 19–27
www.jcb.org/cgi/doi/10.1083/jcb.201108124

Results and discussion

Systematic analysis of NPC ubiquitylation

To analyze systematically modification of the NPC by ubiquitin, we generated a library of strains expressing a genomically HA-tagged version of each Nup. Expression of an inducible His-tagged version of ubiquitin in each of these strains allowed the purification of corresponding cellular ubiquitylated proteins on nickel columns and subsequent Western blotting analysis to detect ubiquitylated HA-tagged Nups (Vitaliano-Prunier et al., 2008). This systematic approach revealed that 6 out of 12 Nups containing FG repeats were conjugated with ubiquitin, with four FG-Nups being essentially monoubiquitylated. We found no correlation between modification and localization of Nups within the NPC (Fig. 1, A and C; and Fig. S1). In contrast, none of the trans-membrane proteins anchoring the NPC in the nuclear envelope was modified, suggesting that accessibility for the conjugation machinery is required for ubiquitylation to occur (Fig. 1, B and C). The complete analysis of every Nups reveals that at least half of the Nups harbor a modification by ubiquitin, either a monoubiquitylation or a pluriubiquitylation corresponding to either a ubiquitin chain or distinct monoubiquitylated sites (Fig. 1 C, Fig. S1, and Fig. S2). Our present results not only validate but also expand previous hits from high-throughput datasets on specific Nups (Nup84, Nup145, Nup120, Nup157, Nup60, and Nic96; Hitchcock et al., 2003; Peng et al., 2003). In addition, extensive analysis of NPC ubiquitylation clearly shows that the ubiquitylation profiles of the yeast Nups are highly variable, suggesting that ubiquitylation of the NPC is not simply related to proteasome-dependent protein turnover or misfolding but might be associated with broader functions of the NPC.

Nup159 is ubiquitylated on lysine K897 by a Cdc34 and SCF-dependent pathway

To assess the function of ubiquitin modification of the NPC, we focused our attention on Nup159, a FG-Nup located exclusively on the cytoplasmic side of the NPC. Besides its central FG repeat domain involved in the interaction with nuclear transport receptors, Nup159 contains an N-terminal domain required for binding to the DEAD box protein Dbp5 (important for the terminal steps of mRNA nuclear export) as well as a C-terminal coiled-coil domain involved in the assembly of the Nup82–Nup159–Nsp1 complex and NPC organization (Del Priore et al., 1997; Belgareh et al., 1998; Weirich et al., 2004). Between these N- and C-terminal domains, Nup159 contains a tandem of six consensus binding motifs for dynein light chain (Dyn2) that mediates the functional interaction of Dyn2 with the NPC (Fig. 2 A; Stelter et al., 2007). Dyn2 was proposed to promote dimerization of the Nup82–Nup159–Nsp1 complex and to stabilize its incorporation into the NPC (Stelter et al., 2007). A recent large-scale proteomic study identified, by mass spectrometry, the lysine residue 897 (K897) of Nup159 as an ubiquitylation site, which is dependent on the F-box protein Grr1 (Radivojac et al., 2010). Mutation of K897 into arginine strongly affected the ability of *nup159K897R*-HA to be modified in vivo, thus confirming that K897 represents the major ubiquitylation site (Fig. 2 B). The residual monoubiquitylation of *nup159K897R* could result either from an alternative ubiquitylation site or a ubiquitylation site artificially unmasked by the K897R mutation. Mutation of K897 did not affect the expression level of Nup159, indicating that ubiquitylation of Nup159 is probably not involved in targeting this Nup to the proteasome-mediated degradation pathway (Fig. 2 B). Accordingly, turnover measurements assessed by cycloheximide chase experiments indicate that both Nup159 and its ubiquitylated form are highly stable (unpublished data). Grr1 is one of the adaptor subunits that recruit specific substrates to the SCF (for Skp1–Cdc53–F-box) E3 ligase, which in turn specifically recruits the Cdc34-conjugating enzyme (Skowyra et al., 1997). Analysis of a thermosensitive mutant of Cdc34 indicated that ubiquitylation of Nup159 is controlled by Cdc34 and SCF (Fig. 2 C). It is unclear whether ubiquitylation of Nup159 is directly catalyzed by the Cdc34/SCF enzymes or results from an indirect Cdc34/SCF-dependent ubiquitylation pathway. However, the presence of the $STVS^{889}$ motif and S889 phosphorylation eight residues downstream of K897 suggests that Grr1 may directly recognize Nup159 (Albuquerque et al., 2008). Because of the pleiotropic effects of both SCF and Cdc34, we analyzed the role of Nup159 modification essentially using the K897R mutant.

Ubiquitylation of Nup159 controls the ability of Nup159 to recruit the dynein light chain to the NPC

To unravel the function of Nup159 ubiquitylation, we first analyzed the consequences of posttranslational modification on Nup159 localization and NPC distribution. For this purpose, wild-type (wt) and mutant forms of Nup159 were genomically tagged with mCherry in strains expressing a GFP-tagged version of Nup60, a Nup exclusively located on the nucleoplasmic face of the NPC. To gain a spatial resolution sufficient to distinguish both Nups, high-resolution structured illumination microscopy (SIM) was used to analyze fixed spheroplasts (Gustafsson et al., 2008). This approach allowed us to differentiate Nup60-GFP from Nup159-mCherry (Fig. 2 D), with an apparent distance between the centroids of fluorescence spots of ∼90 nm, consistent with the previously estimated distance of ∼50 nm and confirming their relative distribution within the NPC (Rout et al., 2000; Alber et al., 2007). Preventing ubiquitylation of Nup159 did not alter the relative localization with respect to Nup60 (Fig. 2 D) or the overall NPC distribution as visualized by expression of Nup49-GFP or Nup159-GFP (Fig. S3, A and B). Although Nup159 plays an essential role in mRNA export through its ability to recruit Dbp5, FISH assay using oligo-dT probes did not reveal any significant export defect in *nup159K897R*-expressing cells (Fig. S3 C), consistent with the absence of any growth defect in these cells at different temperatures (from 23 to 39°C; unpublished data). In contrast, the targeting of genomically tagged

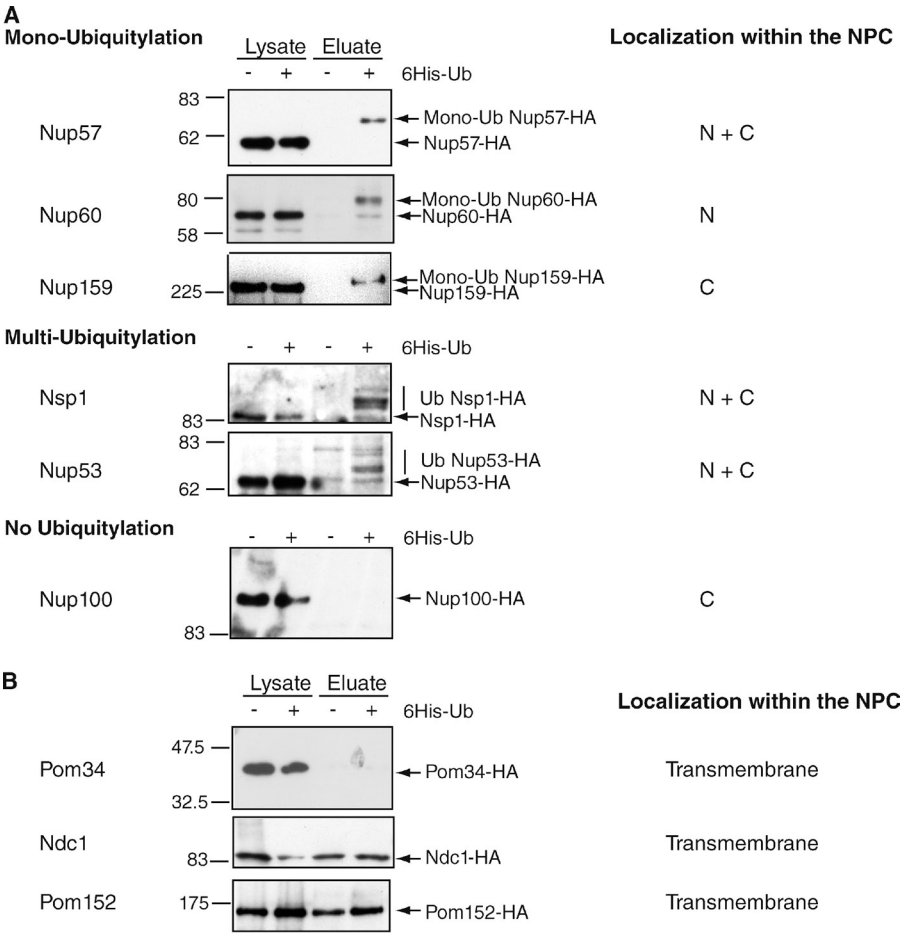

C

FG-repeat proteins	
Nup42	No
Nup49	No
Nup53	mono-ub
Nup57	mono-ub
Nup59	No
Nup60	mono-ub
Nup145N	-
Nsp1	multi-ub
Nup116	multi-ub
Nup1	No
Nup100	No
Nup159	mono-ub
Membrane Proteins	
Pom34	No
Ndc1	No
Pom152	No

Nup84 Complex	
Sec13	mono-ub
Seh1	mono-ub
Nup145C	multi-ub
Nup84	multi-ub
Nup85	No
Nup120	mono-ub
Nup133	mono-ub
Nup170 Complex	
Nup157	mono-ub
Nup170	mono-ub
Nup188	No
Nup192	No
Linker Proteins	
Nup82	multi-ub
Nic96	mono-ub
Others	
Gle2	No
Gle1	No

Figure 1. **Ubiquitylation of nucleoporins.** Ni-purified 6His-ubiquitin (Ub)–conjugated forms of genomically HA-tagged Nups were extracted from cells transformed (+) or not transformed (−) with a plasmid encoding 6His-ubiquitin under control of the *CUP1* promoter. Cell lysates and Ni-purified material were examined by Western blotting with an anti-HA antibody. Ubiquitin expression and efficiency of purification were controlled using an anti-6His antibody (not depicted). Localization of Nups as previously determined (Rout et al., 2000) is indicated on the right (N, nuclear side of the NPC; C, cytoplasmic side of the NPC). (A) Analysis of ubiquitin-conjugated forms of genomically HA-tagged FG-Nups. (B) Analysis of ubiquitin-conjugated forms of genomically HA-tagged transmembrane Nups. (C) Summary of the ubiquitylation status of Nups. Molecular masses are given in kilodaltons.

Dyn2-GFP to the NPC was severely affected in *nup159K897R* mutant cells, with Dyn2-GFP mainly associated with cytoplasmic structures previously identified as peroxisomes as well as foci colocalizing with the dynein complex (Fig. 2 E; Stelter et al., 2007; Stuchell-Brereton et al., 2011). To rule out a conformational effect caused by the K897R mutation, localization of Dyn2-GFP was analyzed in a *cdc34* thermosensitive mutant. The shift from the permissive to the restrictive temperature also led to loss of Dyn2-GFP at the NPC in *cdc34ts* cells but not in wt cells (Fig. 2 E and not depicted). Similarly, localization of Dyn2-GFP at the NPC was strongly decreased in *Δgrr1* cells (unpublished data). Together these results indicate that SCF-mediated ubiquitylation of Nup159 on K897, a residue located at the vicinity of the dynein-binding

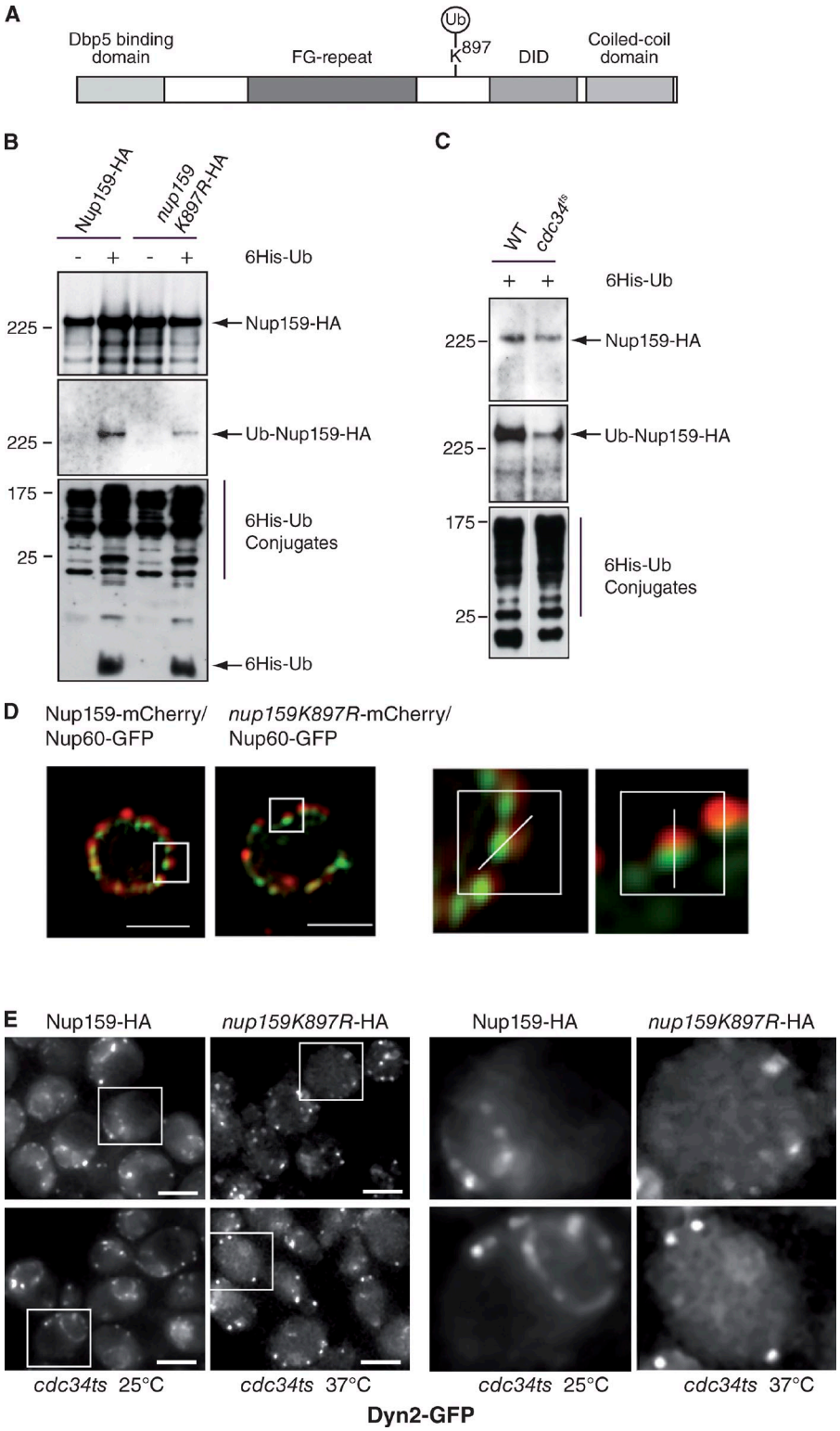

Figure 2. **Ubiquitylation of Nup159 and its role in Dyn2 localization at the NPC.** (A) Schematic representation of Nup159 molecular organization (DID, dynein-interacting domain). (B) Ni-purified 6His-ubiquitin (Ub)–conjugated forms of Nup159-HA were extracted from cells transformed (+) or not transformed (−) with a plasmid encoding 6His-ubiquitin under control of the *CUP1* promoter. Cell lysates (top) and Ni-purified material (middle) were examined by Western blotting with an anti-HA antibody. A portion of the Ni-purified material also was examined by Western blotting on a separate membrane using an anti-6His antibody to show purification efficiency (bottom). (B and C) Analysis of ubiquitin-conjugated forms of Nup159-HA was performed in wt (Nup159-HA) and *nup159K897R*-HA cells (B) and in wt and *cdc34ts* strains (C). The white line indicates that intervening lanes have been spliced out. Molecular markers are given in kilodaltons. (D) Localization of genomically tagged Nup60-GFP and Nup159-mCherry (left) or Nup60-GFP and *nup159K897R*-mCherry was monitored by SIM. Centroid distances of ∼90 ± 20 nm, along the line axis indicated in the magnified areas, were estimated between the two fluorescent signals at the NPC (n = 20 for each cell types). Bars, 1 µm. (E) Localization of genomically tagged Dyn2-GFP was analyzed in Nup159-HA and *nup159K897R*-HA cells as well as in *cdc34ts* cells at 23°C and after a shift to 37°C. NPC localization corresponds to the rimlike staining. The magnified areas (boxes) are shown on the right. Bars, 5 µm.

domain in the primary sequence but not within this domain, control the ability of Nup159 to recruit the dynein light chain to the NPC in vivo. Although the stoichiometry of Nup159 ubiquitylation cannot be precisely quantified as a result of the extreme instability and dynamics of the ubiquitin conjugation and deconjugation processes, 2D gel electrophoresis analysis suggested that one Nup159 copy per NPC might be ubiquitylated (unpublished data). In addition, a previous structural study on complexes formed by Dyn2 and the dynein interaction domain of Nup159 suggested that five stacked Dyn2 homodimers interact with dimers of Nup159 (Stelter et al., 2007). These semiquantitative data would thus support ubiquitylation of Nup159 as being a stoichiometric regulator of dynein binding.

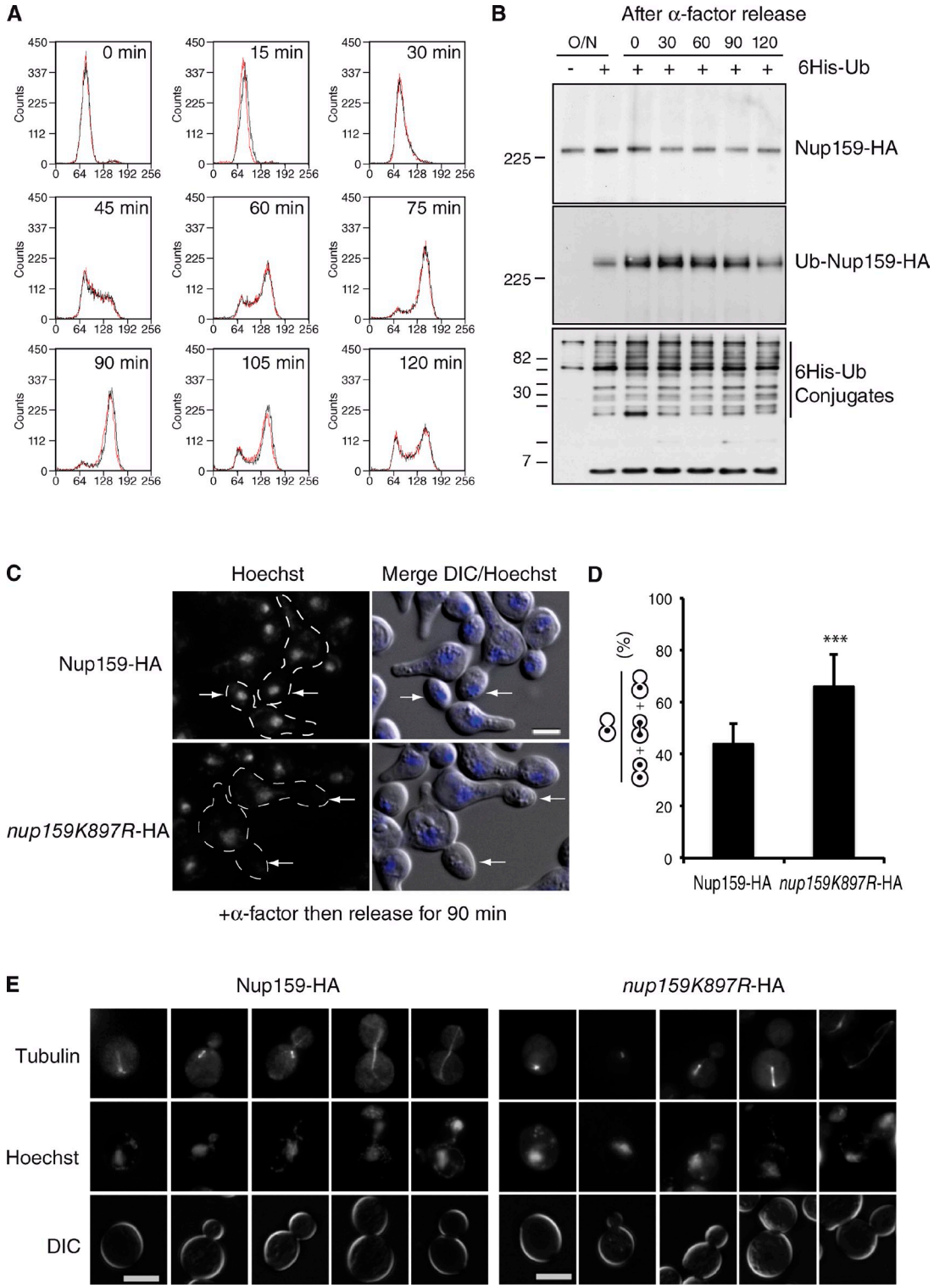

Figure 3. **Ubiquitylation of Nup159 facilitates nuclear migration to the daughter cells during mitosis.** (A) Ubiquitylation of Nup159 does not affect cell cycle progression. Nup159-HA (black) and *nup159K897R*-HA (red) cells were synchronized with α-factor and then released for the indicated period of time before fixation and staining with SYTOX green and analyzed by flow cytometry. Numbers on the bottoms show fluorescence intensity (arbitrary units). (B) Ubiquitylation of Nup159 is not cell cycle dependent. Ni-purified 6His-ubiquitin (Ub)–conjugated forms of Nup159-HA were extracted from unsynchronized (O/N, overnight) cells or from cells treated with α-factor for 3 h before release for indicated periods of time. Cell lysates (top) and Ni-purified material (middle) were examined by Western blotting with an anti-HA antibody. (bottom) Ubiquitin expression and efficiency of purification were controlled using an anti-6His antibody. Molecular markers are given in kilodaltons. Numbers at the top are in minutes. (C) Cells were treated with α-factor for 3 h, released for 90 min, fixed, and stained with Hoechst before epifluorescence and interferential contrast analysis. Dotted lines show the yeast cell contours. Arrows indicate daughter cells. (D) Segregation of nuclei observed in A was analyzed in >100 wt and mutant cells per experiment, and results were obtained from five independent experiments. Error bars show standard deviations. ***, $P < 0.05$. (E) Localization of microtubules was analyzed by fluorescence microscopy in Nup159-HA and *nup159K897R*-HA cells using Tub1-GFP. DIC, differential interference contrast. Bars, 5 μm.

Table 1. **Quantification of the nuclear migration defect**

Strain	Dividing cells with the nucleus only in the mother cell	Number of dividing cells
	%	
NUP159-HA	28 ± 4	260
nup159K897R-HA	46 ± 0**	198
DYN2	21 ± 14	341
dyn2Δ	44 ± 6*[a]	388
NUP159	0.54 ± 0.47	472 at 23°C and 557 at 37°C
nup159-1	1.64 ± 0.27*	440 at 23°C and 375 at 37°C

Asynchronous population of ethanol-fixed cells of the indicated phenotype were stained with Hoechst and analyzed by fluorescence microscopy for the position of the nucleus. Cells whose buds size reached the dividing size (dividing cells) were scored for the presence of nucleus only in the mother cell. For each strain, the number of divided cells counted is indicated in the right column. One asterisk corresponds to p-values between 0.01 and 0.05, and two asterisks correspond to p-values between 0.001 and 0.01.

[a]Value at 37°C normalized to value at 23°C.

Ubiquitylation of Nup159 participates in the dynein-mediated nuclear segregation pathway

The unique function of dynein described so far in *Saccharomyces cerevisiae* is to promote a proper mitotic spindle orientation and position the nucleus at the bud neck during cell division (Eshel et al., 1993; Li et al., 1993; Grava et al., 2006). To determine whether ubiquitylation of Nup159 could be involved in cell cycle progression, Nup159 and *nup159K897R* mutant cells were synchronized in G1 with α-factor, and the DNA content was monitored by FACS analysis after α-factor release. This approach did not reveal defects in the kinetics of cell cycle progression in *nup159K897R* mutant cells (Fig. 3 A). Ubiquitylation of Nup159 appeared slightly more efficient in synchronized cells compared with unsynchronized cells with appearance of a weak additional modified band, but overall, modification of Nup159 was not significantly affected during the cell cycle (Fig. 3 B). Because dynein is required for mitotic spindle and nuclear positioning at the onset of anaphase, and thus impacts the fidelity of nuclear segregation during mitosis, we analyzed the consequences of Nup159 ubiquitylation and Dyn2 delocalization from the NPC during mitosis. Nuclei of cells exhibiting a 2C DNA content (accumulated by synchronization with α-factor and 90-min release) were stained with Hoechst and analyzed by fluorescence microscopy. Under this experimental condition, 66% of nuclei from *nup159K897R* mutant cells did not yet segregate compared with 44% in the wt strain (Fig. 3, C and D). This defect was confirmed in nonsynchronized *nup159K897R* mutant cells as well as in a thermosensitive mutant of Nup159, indicating that Nup159 ubiquitylation can control nuclear migration at the onset of mitosis (Table 1). Deletion of *DYN2* also led to deficient dynein-dependent spindle positioning and nuclear segregation (Table 1; Stuchell-Brereton et al., 2011). Accordingly, preventing Nup159 ubiquitylation results in an alteration of spindle positioning (Fig. 3 E). Together, these results suggest that the ability of Nup159 to target Dyn2 to the pore might be part of the dynein-mediated spindle orientation and nuclear segregation pathway.

In *S. cerevisiae*, the correct orientation of the spindle with the mother–bud axis and consequent nuclear segregation is not only ensured by the dynein–dynactin-mediated pathway but also by a partially redundant pathway using the adenomatous polyposis coli–related protein Kar9 and its partners Bim1 and the type V myosin Myo2 (Miller and Rose, 1998; Korinek et al., 2000; Lee et al., 2000; Hwang et al., 2003). To confirm that ubiquitylation of Nup159 facilitates nuclear segregation via the dynein pathway, we analyzed growth and nuclear segregation phenotypes in double mutant strains containing a *KAR9* deletion in combination with either wt Nup159 or *nup159K897R*. Mutation of the ubiquitylation site of Nup159 induced a severe growth defect in the *kar9Δ* genetic background at 37°C compared with single mutants. In contrast, no growth phenotype was observed when *nup159K897R* mutation was combined with deletion of the dynein heavy chain gene *DYN1* (Fig. 4 A). We thus analyzed nuclear positioning in the *kar9Δ nup159K897R* cells at 30°C and found that they already exhibited a serious defect in nuclear segregation, cytokinesis, and polarity at 30°C (Fig. 4 B). In contrast to the double mutant, the *nup159K897R* cells expressing the Kar9 protein displayed a normal phenotype (unpublished data). The synthetic effect of *KAR9* deletion and *nup159K897R* mutation clearly confirms that ubiquitylation of Nup159 corresponds to an essential event of the dynein pathway.

Our results clearly indicate that NPC is extensively modified by ubiquitin conjugation, and the diversity of the ubiquitylation profiles suggests that targeting to the proteasome-mediated degradation is not the unique function of these modifications. As exemplified by our study on Nup159, the detailed analysis of Nup ubiquitylation likely offers a tool to unravel functions of Nups whose study is often masked by the essential role of the NPC in nuclear transport. In particular, our results lead us to propose that the NPC is directly involved in the nucleus segregation in *S. cerevisiae*, likely by participating in the dynein–dynactin pathway. Interestingly, human Nup133 was recently involved in anchoring the dynein–dynactin complex at the NPC in prophase, a mechanism that contributes to the tethering of centrosomes at the nuclear envelope (Bolhy et al., 2011). In many organisms, effective nuclear positioning and migration rely on the recruitment of different motors, including dynein or kinesins, at the nuclear envelop through interaction with Nups, such as RanBP2, or SUN-KASH domain proteins (Tanenbaum et al., 2011). Deciphering the ubiquitylation pattern of the NPC reveals

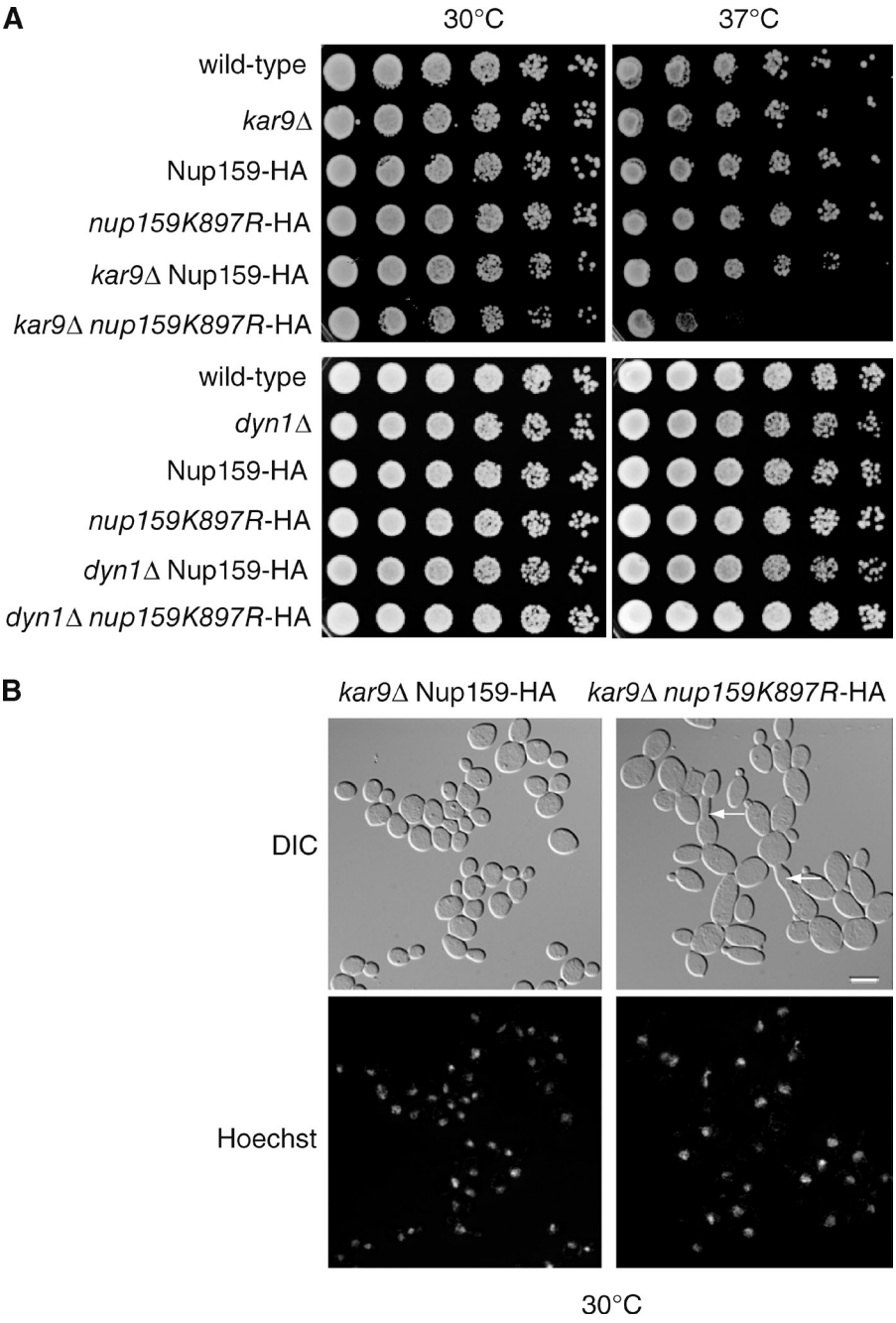

Figure 4. **Ubiquitylation of Nup159 is in the dynein pathway not the Kar9 pathway.** (A) Serial dilutions of the corresponding strains were spotted onto YPD plates and grown at the indicated temperature. (B) *kar9Δ*Nup159-HA and *kar9Δnup159K897R*-HA cells grown at 30°C were fixed and stained with Hoechst before epifluorescence and interferential contrast analysis. Arrows indicate some defecting cells. DIC, differential interference contrast. Bar, 5 µm.

that this evolutionarily conserved function of the NPC in higher eukaryotes is already exploited in the yeast *S. cerevisiae* and may open other new avenues on yet-unidentified functions of the NPC.

Materials and methods

Strains and plasmids

The p415-Nup159-HA plasmid was constructed by PCR amplification of the genomic DNA fragment encoding Nup159-HA and cloning in SpeI–XhoI sites. The plasmid encoding Nup159K897R was constructed from p415-Nup159-HA by site-directed mutagenesis using the site-directed mutagenesis kit (QuickChange; Agilent Technologies). These plasmids were transformed into the W303 MATa *bar1Δ* strain before deleting the *NUP159* chromosomal copy. To combine *KAR9* deletion with *NUP159* mutation, W303 *MATa* Δkar9 and W303 *MATα Δnup159 Nup159-HA* or W303 *MATα Δnup159 nup159K897R*-HA cells were streaked on a dropout Leu with G418 plate and incubated at 30°C for 2 d. Diploids were incubated with sporulation buffer (1% potassium acetate, 0.1% yeast extract, and 0.05% glucose) supplemented with the required amino acids at 30°C for 5 d to induce sporulation. After sporulation, a small path of cells was transferred to 100 µl H_2O and 5 µl Zymolyase (20T; 20 mg/ml) and incubated at 37°C for 5 min. Dissected spores were plated on YPAD (YPD [yeast peptone dextrose] + adenine) plate for 3 d, and their genotypes were analyzed by replicating on appropriate media. Other strains used in this paper are described in Table 2 and Table 3.

Purification of ubiquitylated proteins

Cells transformed with a plasmid encoding 6His-ubiquitin under the *CUP1* promoter were grown on selective media and stimulated overnight with 0.1 mM $CuSO_4$. 100 OD_{600} of cells were lysed in 6 M guanidinium–HCl, 0.1 M Na_2HPO_4/NaH_2PO_4, 0.01 M Tris–HCl, pH 8.0, 0.1% Triton X-100 plus 5 mM imidazole, 10 mM β-mercaptoethanol, protease inhibitors, 20 mM *N*-ethylmaleimide, and 100 µM MG132. Purifications were performed on Ni^{2+}-nitrilotriacetic acid–agarose beads prewashed with

Table 2. **Strains used in this study**

Strain	Genotype
MT670	*MATa ade2 his3 leu2 trp1 ura3 cdc34-2*
MT670 *NUP159-HA*	MT670 *NUP159-3HA::hphNT1*
W303 *NUPX-HA*	*MATα nupx-3HA::HIS3MX6*
W303Δ*bar1*	*MATa bar1::URA3*
W303Δ*bar1 Nup159-HA*	*MATa bar1::URA3NUP159-3HA::hphNT1*
W303Δ*bar1*Δ*nup159 Nup159-HA*	*MATa bar1::URA3 nup159::hphNT1 p415ADH Nup159-HA*
W303Δ*bar1*Δ*nup159nup159K897R*-HA	*MATa bar1::URA3 nup159::hphNT1 p415ADH nup159K897R*-HA
W303Δ*bar1*Δ*nup159 DYN2-GFP Nup159-HA*	*MATa bar1::URA3 nup159::hphNT1 Nup159-HA DYN2- GFP*::KanMX4
W303Δ*bar1*Δ*nup159DYN2-GFP,nup159K897R*-HA	*MATa bar1::URA3 nup159::hphNT1 nup159K897R*-HA *DYN2-GFP*::KanMX4
BY4741 *NUP60-GFP NUP159-mCherry*	BY4741 *nup60-GFP::HIS3MX6 nup159-mCherry*::KanMX
BY4741 *NUP60-GFP NUP159K897R-mCherry*	BY4741*nup60-GFP::HIS3MX6nup159K897R-mCherry*::KanMX
W303Δ*kar9*Δ*nup159 Nup159-HA*	*MAT? kar9::KanMX4 nup159::hphNT1 p415ADH Nup159-HA*
W303Δ*kar9*Δ*nup159 nup159K897R*-HA	*MAT? kar9::KanMX4 nup159::hphNT1 p415ADH nup159K897R*-HA
BY4741 *DYN2-GFP*	BY4741 *DYN2-GFP::HIS3MX6*
BY4741 *DYN2-GFP grr1Δ*	BY4741 *DYN2-GFP::HIS3MX6* grr1Δ::KanMX
W303Δ*nup159 Nup159-HA* Cdc10-mCherry	*MATα CDC10-mCherry*::KanMX4*nup159::hphNT1 p415ADH Nup159-HA*
W303Δ*nup159 nup159K897R*-HA Cdc10-mCherry	*MATα CDC10-mCherry*::KanMX4*nup159::hphNT1 p415ADH nup159K897R*-HA
MT670 Nup159-mCherry	*MATa ade2his3leu2trp1ura3cdc34-2NUP159*-mCherry::KanMX4

lysis buffer and incubated for 2 h at room temperature. The beads were washed with 8 M urea, 0.1 M Na_2HPO_4/NaH_2PO_4, 0.01 M Tris–HCl, pH 6.3, 10 mM β-mercaptoethanol, and 0.2% Triton X-100 before elution and Western blot analysis using anti-HA and anti-His6 antibodies (Vitaliano-Prunier et al., 2008). For the time course experiment, cells were first lysed and precipitated in TCA before purification of ubiquitylated proteins as previously described in Ziv et al. (2011).

Flow cytometry analysis

Yeast cells were synchronized by treatment with 50 ng/ml α-factor for 3 h before washing. One million cells per condition were fixed in 70% ethanol overnight, treated overnight with 0.1 mg/ml RNase A at 37°C and 5 mg/ml pepsin for 20 min at 37°C, and then stained with 10 µM SYTOX green (Invitrogen) before flow cytometry analysis (Babour et al., 2010).

High-resolution SIM

For SIM, yeast cells coexpressing genomically tagged Nup60-GFP and wt or a K897R mutant of Nup159-mCherry were fixed in 4% PFA. Spheroplasts were obtained with 0.5 µg/µl Zymolyase 100T and mounted on poly-L-lysine–coated coverslips. Acquisitions were performed in 2D SIM mode with a microscope (N-SIM; Nikon) before image reconstruction using the NIS-Elements software (Nikon; based on Gustafsson et al., 2008). The system is equipped with an Apochromat total internal reflection fluorescence 100× 1.49 NA oil immersion, a laser illumination (488 nm at 200 mW and 561 nm at 100 mW), and an EM charge-coupled device camera (DU-897; Andor).

Fluorescence microscopy

Yeast cells were fixed with 70% ethanol and stained with Hoechst 33342. Cdc34 mutant cells expressing genomically tagged Dyn2-GFP were incubated at 25°C overnight and shifted to 37°C for 2 h before fixation. Wide-field fluorescence images were acquired using a microscope (DMR; Leica) with a 100× Plan Apochromat HCX oil immersion objective and a high-sensitivity cooled interlined charge-coupled device camera (CoolSNAP HQ2; Photometrics). Rapid and precise z positioning was accomplished by a piezoelectric motor (LVDT; Physik Instrumente) mounted underneath the objective lens. Maximum intensity projections were performed using MetaMorph software (Universal Imaging Corp.). Denoising using the nD-Safir software was performed on all original images (Boulanger et al., 2010). Identical processing parameters and number of iterations were used.

Statistical analysis

Significance of the differences observed for recruitment between wt and mutant cells was evaluated using Student's *t* test. No asterisk corresponds to $P > 0.05$, one asterisk corresponds to p-values between 0.01 and 0.05, and two asterisks correspond to p-values between 0.001 and 0.01.

Online supplemental material

Fig. S1 shows ubiquitylation of FG-Nups and Nup84 subcomplex. Fig. S2 shows ubiquitylation of linker Nups, Nup170 subcomplex, Gle1, and Gle2. Fig. S3 shows that ubiquitylation of Nup159 does not control NPC distribution nor mRNA nuclear export. Online supplemental material is available at http://www.jcb.org/cgi/content/full/jcb.201108124/DC1.

We are most grateful to J. Salamero, R. Karess, L. Pintard, V. Doye, H. De Thé, and J. Weitzmann for very helpful discussions and critical reading of the manuscript as well as to C. Nino Suarez for his assistance in some experiments.

This study was funded by grants from the Agence Nationale pour la Recherche (2010 BLAN1227-01 to C. Dargemont) and the Ligue contre le Cancer (C. Dargemont is Equipe Labellisée). A. Hayakawa and A. Babour are supported by the Fondation pour la Recherche Médicale and the Association de Recherche contre le Cancer, respectively.

Submitted: 22 August 2011
Accepted: 6 December 2011

Table 3. **Plasmids used in this study**

Plasmid Name	Marker	Promoter	Expressed protein
p415 ADH Nup159-HA	*LEU2*	*ADH*	Nup159-3HA
p415 ADH Nup159K897R-HA	*LEU2*	*ADH*	Nup159K897R-3HA
AFS125-TUB1-GFP	*URA3*	*TUB1*	Tub1-GFP
pFL38-GFP-Nup49	*URA3*	*5′NUP49*	GFP-Nup49

ADH, alcohol dehydrogenase.

References

Alber, F., S. Dokudovskaya, L.M. Veenhoff, W. Zhang, J. Kipper, D. Devos, A. Suprapto, O. Karni-Schmidt, R. Williams, B.T. Chait, et al. 2007. The molecular architecture of the nuclear pore complex. *Nature*. 450:695–701. http://dx.doi.org/10.1038/nature06405

Albuquerque, C.P., M.B. Smolka, S.H. Payne, V. Bafna, J. Eng, and H. Zhou. 2008. A multidimensional chromatography technology for in-depth phosphoproteome analysis. *Mol. Cell. Proteomics*. 7:1389–1396. http://dx.doi.org/10.1074/mcp.M700468-MCP200

Babour, A., A.A. Bicknell, J. Tourtellotte, and M. Niwa. 2010. A surveillance pathway monitors the fitness of the endoplasmic reticulum to control its inheritance. *Cell*. 142:256–269. http://dx.doi.org/10.1016/j.cell.2010.06.006

Belgareh, N., C. Snay-Hodge, F. Pasteau, S. Dagher, C.N. Cole, and V. Doye. 1998. Functional characterization of a Nup159p-containing nuclear pore subcomplex. *Mol. Biol. Cell*. 9:3475–3492.

Bolhy, S., I. Bouhlel, E. Dultz, T. Nayak, M. Zuccolo, X. Gatti, R. Vallee, J. Ellenberg, and V. Doye. 2011. A Nup133-dependent NPC-anchored network tethers centrosomes to the nuclear envelope in prophase. *J. Cell Biol.* 192:855–871. http://dx.doi.org/10.1083/jcb.201007118

Boulanger, J., C. Kervrann, P. Bouthemy, P. Elbau, J.B. Sibarita, and J. Salamero. 2010. Patch-based nonlocal functional for denoising fluorescence microscopy image sequences. *IEEE Trans. Med. Imaging*. 29:442–454. http://dx.doi.org/10.1109/TMI.2009.2033991

Chakraborty, P., Y. Wang, J.H. Wei, J. van Deursen, H. Yu, L. Malureanu, M. Dasso, D.J. Forbes, D.E. Levy, J. Seemann, and B.M. Fontoura. 2008. Nucleoporin levels regulate cell cycle progression and phase-specific gene expression. *Dev. Cell*. 15:657–667. http://dx.doi.org/10.1016/j.devcel.2008.08.020

Cronshaw, J.M., A.N. Krutchinsky, W. Zhang, B.T. Chait, and M.J. Matunis. 2002. Proteomic analysis of the mammalian nuclear pore complex. *J. Cell Biol.* 158:915–927. http://dx.doi.org/10.1083/jcb.200206106

Del Priore, V., C. Heath, C. Snay, A. MacMillan, L. Gorsch, S. Dagher, and C. Cole. 1997. A structure/function analysis of Rat7p/Nup159p, an essential nucleoporin of *Saccharomyces cerevisiae*. *J. Cell Sci.* 110:2987–2999.

Eshel, D., L.A. Urrestarazu, S. Vissers, J.C. Jauniaux, J.C. van Vliet-Reedijk, R.J. Planta, and I.R. Gibbons. 1993. Cytoplasmic dynein is required for normal nuclear segregation in yeast. *Proc. Natl. Acad. Sci. USA*. 90:11172–11176. http://dx.doi.org/10.1073/pnas.90.23.11172

Glavy, J.S., S.B. Horwitz, and G.A. Orr. 1997. Identification of the in vivo phosphorylation sites for acidic-directed kinases in murine mdr1b P-glycoprotein. *J. Biol. Chem.* 272:5909–5914. http://dx.doi.org/10.1074/jbc.272.9.5909

Glavy, J.S., A.N. Krutchinsky, I.M. Cristea, I.C. Berke, T. Boehmer, G. Blobel, and B.T. Chait. 2007. Cell-cycle-dependent phosphorylation of the nuclear pore Nup107-160 subcomplex. *Proc. Natl. Acad. Sci. USA*. 104:3811–3816. http://dx.doi.org/10.1073/pnas.0700058104

Grava, S., F. Schaerer, M. Faty, P. Philippsen, and Y. Barral. 2006. Asymmetric recruitment of dynein to spindle poles and microtubules promotes proper spindle orientation in yeast. *Dev. Cell*. 10:425–439. http://dx.doi.org/10.1016/j.devcel.2006.02.018

Gustafsson, M.G., L. Shao, P.M. Carlton, C.J. Wang, I.N. Golubovskaya, W.Z. Cande, D.A. Agard, and J.W. Sedat. 2008. Three-dimensional resolution doubling in wide-field fluorescence microscopy by structured illumination. *Biophys. J.* 94:4957–4970. http://dx.doi.org/10.1529/biophysj.107.120345

Hitchcock, A.L., K. Auld, S.P. Gygi, and P.A. Silver. 2003. A subset of membrane-associated proteins is ubiquitinated in response to mutations in the endoplasmic reticulum degradation machinery. *Proc. Natl. Acad. Sci. USA*. 100:12735–12740. http://dx.doi.org/10.1073/pnas.2135500100

Hwang, E., J. Kusch, Y. Barral, and T.C. Huffaker. 2003. Spindle orientation in *Saccharomyces cerevisiae* depends on the transport of microtubule ends along polarized actin cables. *J. Cell Biol.* 161:483–488. http://dx.doi.org/10.1083/jcb.200302030

Korinek, W.S., M.J. Copeland, A. Chaudhuri, and J. Chant. 2000. Molecular linkage underlying microtubule orientation toward cortical sites in yeast. *Science*. 287:2257–2259. http://dx.doi.org/10.1126/science.287.5461.2257

Kosako, H., N. Yamaguchi, C. Aranami, M. Ushiyama, S. Kose, N. Imamoto, H. Taniguchi, E. Nishida, and S. Hattori. 2009. Phosphoproteomics reveals new ERK MAP kinase targets and links ERK to nucleoporin-mediated nuclear transport. *Nat. Struct. Mol. Biol.* 16:1026–1035. http://dx.doi.org/10.1038/nsmb.1656

Laurell, E., K. Beck, K. Krupina, G. Theerthagiri, B. Bodenmiller, P. Horvath, R. Aebersold, W. Antonin, and U. Kutay. 2011. Phosphorylation of Nup98 by multiple kinases is crucial for NPC disassembly during mitotic entry. *Cell*. 144:539–550. http://dx.doi.org/10.1016/j.cell.2011.01.012

Lee, L., J.S. Tirnauer, J. Li, S.C. Schuyler, J.Y. Liu, and D. Pellman. 2000. Positioning of the mitotic spindle by a cortical-microtubule capture mechanism. *Science*. 287:2260–2262. http://dx.doi.org/10.1126/science.287.5461.2260

Li, Y.Y., E. Yeh, T. Hays, and K. Bloom. 1993. Disruption of mitotic spindle orientation in a yeast dynein mutant. *Proc. Natl. Acad. Sci. USA*. 90:10096–10100. http://dx.doi.org/10.1073/pnas.90.21.10096

Lusk, C.P., D.D. Waller, T. Makhnevych, A. Dienemann, M. Whiteway, D.Y. Thomas, and R.W. Wozniak. 2007. Nup53p is a target of two mitotic kinases, Cdk1p and Hrr25p. *Traffic*. 8:647–660. http://dx.doi.org/10.1111/j.1600-0854.2007.00559.x

Macaulay, C., E. Meier, and D.J. Forbes. 1995. Differential mitotic phosphorylation of proteins of the nuclear pore complex. *J. Biol. Chem.* 270:254–262. http://dx.doi.org/10.1074/jbc.270.1.254

Miller, R.K., and M.D. Rose. 1998. Kar9p is a novel cortical protein required for cytoplasmic microtubule orientation in yeast. *J. Cell Biol.* 140:377–390. http://dx.doi.org/10.1083/jcb.140.2.377

Onischenko, E.A., N.V. Gubanova, E.V. Kiseleva, and E. Hallberg. 2005. Cdk1 and okadaic acid-sensitive phosphatases control assembly of nuclear pore complexes in *Drosophila* embryos. *Mol. Biol. Cell*. 16:5152–5162. http://dx.doi.org/10.1091/mbc.E05-07-0642

Peng, J., D. Schwartz, J.E. Elias, C.C. Thoreen, D. Cheng, G. Marsischky, J. Roelofs, D. Finley, and S.P. Gygi. 2003. A proteomics approach to understanding protein ubiquitination. *Nat. Biotechnol.* 21:921–926. http://dx.doi.org/10.1038/nbt849

Radivojac, P., V. Vacic, C. Haynes, R.R. Cocklin, A. Mohan, J.W. Heyen, M.G. Goebl, and L.M. Iakoucheva. 2010. Identification, analysis, and prediction of protein ubiquitination sites. *Proteins*. 78:365–380. http://dx.doi.org/10.1002/prot.22555

Rout, M.P., J.D. Aitchison, A. Suprapto, K. Hjertaas, Y. Zhao, and B.T. Chait. 2000. The yeast nuclear pore complex: composition, architecture, and transport mechanism. *J. Cell Biol.* 148:635–651. http://dx.doi.org/10.1083/jcb.148.4.635

Skowyra, D., K.L. Craig, M. Tyers, S.J. Elledge, and J.W. Harper. 1997. F-box proteins are receptors that recruit phosphorylated substrates to the SCF ubiquitin-ligase complex. *Cell*. 91:209–219. http://dx.doi.org/10.1016/S0092-8674(00)80403-1

Stelter, P., R. Kunze, D. Flemming, D. Höpfner, M. Diepholz, P. Philippsen, B. Böttcher, and E. Hurt. 2007. Molecular basis for the functional interaction of dynein light chain with the nuclear-pore complex. *Nat. Cell Biol.* 9:788–796. http://dx.doi.org/10.1038/ncb1604

Stuchell-Brereton, M.D., A. Siglin, J. Li, J.K. Moore, S. Ahmed, J.C. Williams, and J.A. Cooper. 2011. Functional interaction between dynein light chain and intermediate chain is required for mitotic spindle positioning. *Mol. Biol. Cell*. 22:2690–2701. http://dx.doi.org/10.1091/mbc.E11-01-0075

Tanenbaum, M.E., A. Akhmanova, and R.H. Medema. 2011. Bi-directional transport of the nucleus by dynein and kinesin-1. *Commun Integr Biol*. 4:21–25.

Vitaliano-Prunier, A., A. Menant, M. Hobeika, V. Géli, C. Gwizdek, and C. Dargemont. 2008. Ubiquitylation of the COMPASS component Swd2 links H2B ubiquitylation to H3K4 trimethylation. *Nat. Cell Biol.* 10:1365–1371. http://dx.doi.org/10.1038/ncb1796

Weirich, C.S., J.P. Erzberger, J.M. Berger, and K. Weis. 2004. The N-terminal domain of Nup159 forms a beta-propeller that functions in mRNA export by tethering the helicase Dbp5 to the nuclear pore. *Mol. Cell*. 16:749–760. http://dx.doi.org/10.1016/j.molcel.2004.10.032

Ziv, I., Y. Matiuhin, D.S. Kirkpatrick, Z. Erpapazoglou, S. Leon, M. Pantazopoulou, W. Kim, S.P. Gygi, R. Haguenauer-Tsapis, N. Reis, et al. 2011. A perturbed ubiquitin landscape distinguishes between ubiquitin in trafficking and in proteolysis. *Mol. Cell. Proteomics*. 10:M111.009753.